© 2016. Published by The Company of Biologists Ltd | Journal of Cell Science (2016) 129, 1378-1390 doi:10.1242/jcs.178251

RESEARCH ARTICLE

CAPS1 effects on intragranular pH and regulation of BDNF release from secretory granules in hippocampal neurons

Robert Eckenstaler[1], Volkmar Lessmann[1,2,*,‡] and Tanja Brigadski[1,2,*,‡]

ABSTRACT

The secretory protein brain-derived neurotrophic factor (BDNF) is assumed to be a key factor for the induction of synaptic plasticity processes in neurons. However, the molecular mechanisms for activity-dependent release of the protein largely remain elusive. Here, we demonstrate the relevance of the priming factor CAPS1 (also known as CADPS) for the maturation and exocytosis of BDNF-containing secretory granules, as well as for neurotransmitter release from synaptic vesicles. Using live-cell imaging and RNA silencing methods, we show that CAPS1 has a previously unrecognized function in regulating the intragranular pH of BDNF-containing secretory granules. Furthermore, our results demonstrate that acute single-cell knockdown of CAPS1 with unaltered expression in neighboring neurons leads to a strong reduction in the number of fusion-competent secretory granules and to a significant decrease of released BDNF following exocytosis in dendrites of CAPS1-deficient neurons. In addition, our results show a reduction in synaptic vesicle turnover after CAPS1 knockdown without affecting the density of active boutons in hippocampal neurons. Thus, our results reveal new functions of endogenous CAPS1 in the BDNF secretory granule life cycle, thereby representing a new mechanism of neuronal plasticity.

KEY WORDS: Neurotrophin, BDNF, CAPS1, Neuropeptide secretion, Neurotransmitter, Neurotransmitter release, Hippocampus

INTRODUCTION

The neurotrophin brain-derived neurotrophic factor (BDNF) regulates numerous crucial functions in the developing and adult brain, including neuronal survival and synaptic plasticity (Edelmann et al., 2014; Huang and Reichardt, 2001; Klein, 1994; Lessmann and Brigadski, 2009; Park and Poo, 2013). BDNF is stored in secretory granules, which are released either constitutively or in an activity-dependent manner (Brigadski et al., 2005; Dean et al., 2009; Hartmann et al., 2001; Haubensak et al., 1998; Kohara et al., 2001; Lessmann and Brigadski, 2009; Matsuda et al., 2009). The activity-dependent release of BDNF is assumed to be a key element for the induction and expression of synaptic plasticity (Edelmann et al., 2014, 2015). Thus, understanding the molecular mechanisms of BDNF secretory granule exocytosis in neurons is of upmost importance. Similar to neurotransmitter release from synaptic vesicles, BDNF release is a Ca^{2+}-dependent process that comprises sequential priming and fusion of BDNF granules (Lessmann and Brigadski, 2009). Two proteins which have been suggested to play a major role in secretory granule exocytosis are the Ca^{2+}-dependent activator protein for secretion proteins (CAPS1 and CAPS2, also known as CADPS and CADPS2, respectively). CAPS1 is expressed in several brain regions, including the cerebellum, cortex, hippocampus and olfactory bulb (Sadakata et al., 2006; Speidel et al., 2003). In hippocampal neurons, CAPS1 is localized in axons and dendrites (Farina et al., 2015; Sadakata et al., 2006), and is known to affect secretory granule exocytosis in neuroendocrine cells (Grishanin et al., 2004; Speidel et al., 2005, 2008). Beyond that, a few studies have analyzed the role of CAPS1 in neurons. It has been shown very recently that CAPS1 increases the number of fusion-competent neuropeptide Y (NPY)-containing secretory granules in axons (Farina et al., 2015) and regulates synaptic vesicle exocytosis in cultured neurons (Jockusch et al., 2007). Furthermore, immunocytochemical detection has revealed decreased BDNF protein levels in the molecular layer of the cerebellum of conditional CAPS1-knockout mice (Sadakata et al., 2013). Although these data suggest that CAPS1 can regulate exocytosis, the mechanism of action of CAPS1 in neuropeptide release from primary neurons largely remains unknown.

In the present study we analyzed the functional consequences of acute CAPS1 knockdown in primary hippocampal neurons on secretory granule exocytosis and transmitter release from synaptic vesicles. We used single-cell knockdown of CAPS1 rather than global CAPS1 knockout to exclude secondary effects of altered synaptic network function that can be expected by unselective deletion of CAPS1 in all neurons. Our results show a deficit in synaptic vesicle exocytosis by 5 days after acute knockdown of CAPS1 protein. Basal synaptic properties, such as the density of active boutons, remained unaffected. Furthermore, our results demonstrate that endogenous CAPS1 plays an unprecedented crucial role in several distinguishable steps of the life cycle of BDNF secretory granules. Thus, acute knockdown of CAPS1 abrogated intragranular pH regulation. In addition, we observed a strong decrease in the number of fusion-competent secretory granules in dendrites upon CAPS1 knockdown. This effect was accompanied by a significant reduction in BDNF content release from single secretory granules. Importantly, these functions of CAPS1 on fusion pore opening and BDNF release occurred independently from the above mentioned changes in intragranular pH. These data reveal that CAPS1 has three discernible effects on secretory granule release. These effects are a direct consequence of single-cell knockdown of CAPS1 rather than resulting from a changed neuronal network activity that is likely observed after global and complete deletion in CAPS-knockout models.

RESULTS

Reduction of synaptic vesicle exocytosis by CAPS1 knockdown

Most studies investigating the function of CAPS1 have been performed in permeabilized neuroendocrine cells or in cells derived from constitutive CAPS1-knockout or CAPS1 and CAPS2 double-

[1]Institute of Physiology, Medical Faculty, Otto-von-Guericke-University, Magdeburg 39120, Germany. [2]Center of Behavioral Brain Sciences (CBBS), Magdeburg 39120, Germany.
*These authors contributed equally to this work

‡Authors for correspondence (tanja.brigadski@med.ovgu.de; volkmar.lessmann@med.ovgu.de)

Received 30 July 2015; Accepted 8 February 2016

Journal of Cell Science (2016) 129, 1378-1390 doi:10.1242/jcs.178251

knockout animals completely lacking CAPS1. To focus on the relevance of CAPS1 function in individual neurons after acute CAPS1 downregulation, here, we investigated both synaptic vesicle exocytosis and secretory granule release in hippocampal neurons using live-cell imaging and short hairpin RNA (shRNA)-mediated mRNA silencing. This method enables analysis of acute knockdown of a single protein isoform and thus lowers the likelihood of observing secondary side effects caused by developmental alterations in constitutive knockout mice. Especially when studying activity-dependent processes like transmitter and peptide secretion, such network changes following knockout could hamper the interpretation of CAPS1 functions. Therefore, we transfected neurons with a plasmid coding for CAPS1 shRNA and a fluorescent marker protein to allow selection of CAPS1-depleted single neurons for analysis. To validate the knockdown efficiency of endogenous CAPS1 protein, hippocampal neurons were transfected with a vector driving coexpression of mCherry and CAPS1 shRNA or scrambled control shRNA, respectively (Fig. 1A, Fig. S1). A significant reduction of endogenous CAPS1 expression to 35.0±3.7% was evident in hippocampal neurons transfected with CAPS1 shRNA (n=50 cells) compared to control conditions (n=55 cells; mean±s.e.m.; P<0.001, one-way ANOVA) (Fig. 1B). Knockdown of endogenous CAPS1 protein was further validated by analyzing functional consequences of CAPS1 knockdown on neurotransmitter release. To this aim, we studied synaptic vesicle exocytosis in neurons by monitoring FM1-43 dye destaining (Nimmervoll et al., 2013; Ryan et al., 1993) (Fig. 1C–H). Mouse hippocampal neurons transfected with scrambled control shRNA or CAPS1 shRNA plasmids as well as untransfected hippocampal neurons were stained with FM1-43 dye using saturating stimulation with elevated K^+ (see Materials and Methods). Destaining of synaptic boutons containing FM1-43 dye was induced by brief application of elevated (50 mM) K^+-containing solution. The destaining amplitude 100 s after stimulation (Fig. 1F) was significantly reduced by knockdown of CAPS1 (untransfected control, 51.8±1.4%, n=8 cells; scrambled control shRNA, 50.4±1.5%, n=25 cells; CAPS1 shRNA, 36.4±2.3%, n=27 cells; mean±s.e.m.; P<0.002, one-way ANOVA followed by post hoc Tukey test). In addition, the time constant τ of exponential fluorescence decay was significantly increased by CAPS1 knockdown compared to untransfected control (untransfected control, 12.6±1.0 s; control shRNA, 14.8±1.1 s; CAPS1 shRNA, 18.0±1.1 s; mean±s.e.m.; P<0.04, one-way ANOVA followed by post hoc Tukey test). However, the average size, number and intensity of FM1-43 puncta in transfected neurons, taken as a measure of size and density of active boutons, were similar (Fig. S1F–H). Besides the destaining amplitude, we furthermore characterized the FM1-43 loading and destaining of the readily releasable pool (RRP) of transmitter vesicles after CAPS1 knockdown. To do this, we sequentially stained and destained the RRP and the recycling pool of synaptic vesicles with FM1-43 dye using hypertonic sucrose solution and then elevated K^+ solution (compare Pyle et al., 2000). High-K^+-induced destaining of the FM1-43-labeled RRP was related to the fluorescence loss of the total recycling pool (Fig. 1G; Fig. S1K). Again, we observed a significant reduction of the total recycling pool and the RRP after CAPS1 knockdown (Fig. S2I,J). To evaluate whether the RRP in synaptic boutons was changed, we plotted a histogram of the fraction of readily releasable vesicles across individual synaptic boutons and observed a significant increase in the number of synaptic boutons with a small RRP after CAPS1 knockdown (Fig. 1G,H: control shRNA, 89 boutons; CAPS1 shRNA, 99 boutons; P=0.01, χ-squared test; Fig. S1K: control shRNA, n=94; CAPS1 shRNA, n=84; P<0.01, χ-squared test). Taken together, these results reveal that acute knockdown of CAPS1 leads to impaired neurotransmitter release whereas density and FM1-43 loading of transmitter vesicles remain unaffected.

CAPS1 promotes exocytosis of BDNF-containing secretory granules

Neurotransmitter release from synaptic vesicles and activity-dependent protein release from secretory granules coexist in neuronal cells. Both release processes are Ca^{2+}-dependent and share similar sequences of events, like priming and fusion of vesicles. Nevertheless, complex and subtle differences are important for the tight regulation of both processes. To investigate the role of CAPS1 in secretory granule exocytosis in hippocampal neurons, the functional consequences of CAPS1 knockdown on release of BDNF–GFP-containing vesicles were analyzed. In initial experiments, we investigated colocalization of BDNF–GFP with endogenous CAPS1 in dendrites and axons (Fig. S2). These immunocytochemical data revealed that cytosolic CAPS1 that was present in the vicinity of BDNF-containing granules was apparently more pronounced in dendritic than in axonal compartments. Next, we transfected hippocampal neurons with CAPS1-shRNA- or scrambled-control-shRNA-expressing vectors that also contained a BDNF–GFP coding sequence. This assured that all BDNF–GFP-containing neurons additionally expressed the respective shRNA. Density and size BDNF–GFP-containing vesicles were not affected by acute single-cell knockdown of CAPS1 in these networks consisting predominantly of wild-type neurons (Fig. S2). Next, we determined how different steps of secretory granule exocytosis were affected by CAPS1 knockdown. The incidence of fusion events of BDNF–GFP vesicles was analyzed by monitoring the change of intragranular BDNF–GFP-fluorescence intensity in the presence of the fluorescence quencher Bromophenol Blue (BPB) in the extracellular solution (Kolarow et al., 2007). Transfected hippocampal neurons were continuously superfused with 0.3 mM BPB. Images were captured at 5-s intervals. After a brief control period, cells were depolarized with elevated (50 mM) K^+-containing solution. Depolarization-induced fusion events for single secretory granules were detected as loss of intragranular fluorescence due to immediate quenching of intragranular GFP fluorescence by diffusion of BPB through the opened fusion pore (Fig. 2). Importantly, BPB has been shown previously to have no effect on fusion pore opening on its own (data not shown; see Harata et al., 2006; Kolarow et al., 2007). Next, we analyzed the number of single secretory granule fusion events per time interval. To do this, data were binned at 10-s intervals. Most events occurred 10–20 s after stimulation in both knockdown and control cells (Fig. 2D). Although the timecourse of exocytosis, as reflected by the cumulative plot of fusion events, was similar in both groups (Fig. 2E), the absolute number of fusion events was strongly reduced upon CAPS1 knockdown (Fig. 2F, control shRNA, 21.5±3.8%, n=18; CAPS1 shRNA, 9.0±1.2%, n=17; mean±s.e.m.; P<0.01, one-way ANOVA). No regional differences between intermediate dendrites and dendritic endings were evident (Fig. S3A–E). This result was also not dependent on possible CAPS1-induced changes in synaptic transmission, as measurements in the presence of synaptic blockers revealed the same results (Fig. S3F). These results suggest a significant reduction in the number of fusion-competent secretory granules in hippocampal neurons upon CAPS1 knockdown.

Journal of Cell Science (2016) 129, 1378-1390 doi:10.1242/jcs.178251

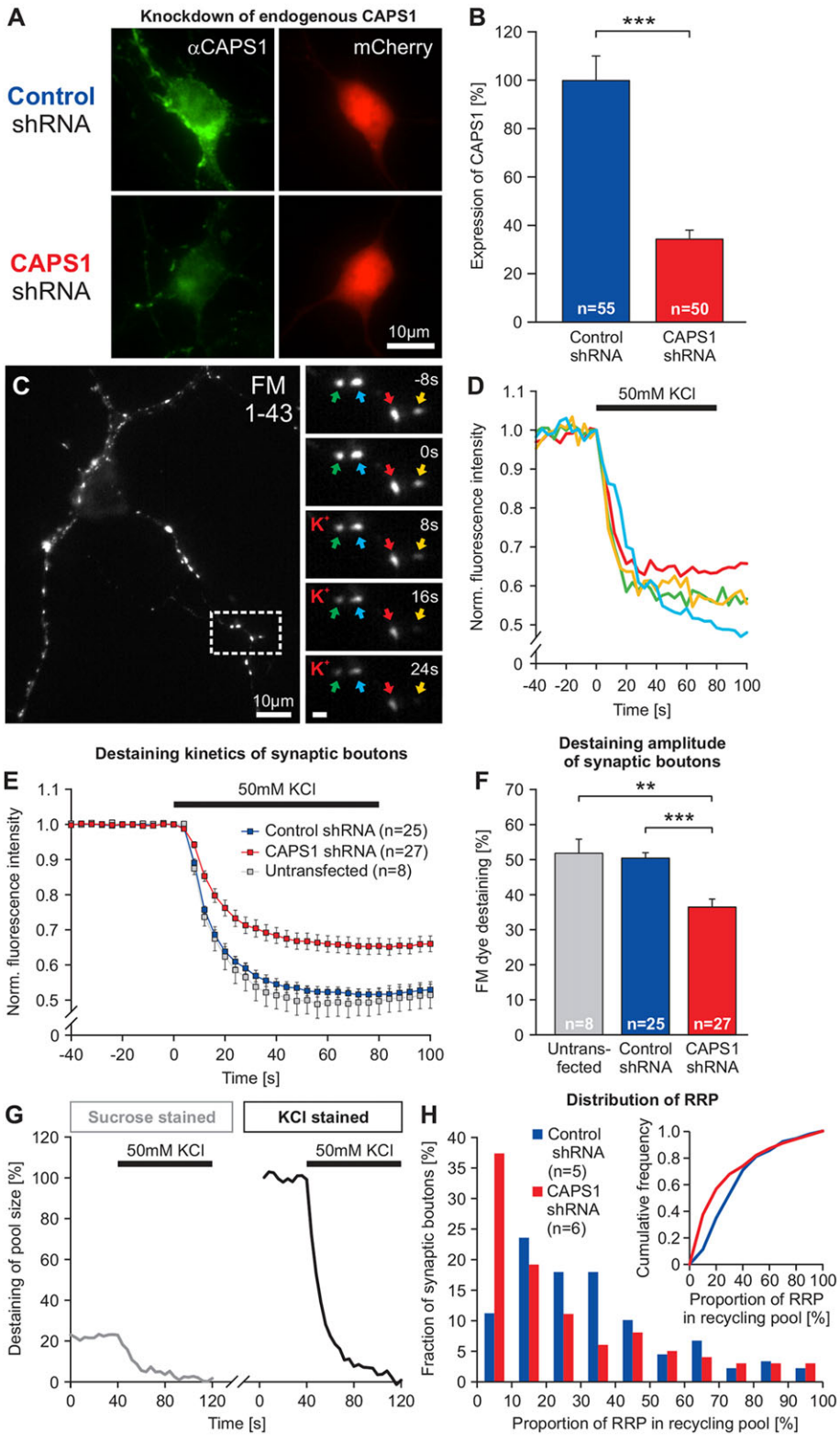

Fig. 1. Deficits in synaptic transmitter vesicle release after CAPS1 knockdown.
(A) Knockdown of CAPS1 expression was evaluated in hippocampal neurons transfected with CAPS1 shRNA or scrambled control shRNA constructs, both enabling coexpression of mCherry as reporter protein to identify transfected cells. Representative pictures of hippocampal neurons immunostained with an antibody directed against endogenous CAPS1 (green) after transfection with CAPS1 shRNA (lower panels) or scrambled control shRNA (upper panels) coexpressing mCherry as reporter protein (red). (B) Fluorescence intensity of fluorophores coupled to secondary antibodies was analyzed in the soma to estimate the expression level of endogenous CAPS1 after shRNA-mediated silencing. The mean anti-CAPS1 fluorescence intensity of hippocampal neurons transfected with CAPS1 shRNA (red) was significantly reduced compared to control-shRNA-transfected cells (blue, set to 100%). (C) FM® 1-43-labeled presynaptic terminals of a representative hippocampal neuron. Neurons were stained with FM® 1-43 dye under high K^+ stimulation (50 mM) and saturating conditions directly prior to destaining measurements. Right, higher magnification of the boxed area. Destaining was induced by depolarization of the neuron with 50 mM K^+ solution at the indicated time points (0 s=start of application). Colored arrows mark example regions which were analyzed in D. (D) Timecourse of relative fluorescence intensity of example regions shown in C. Note the fast decrease in fluorescence intensity after the onset of depolarization. (E) Average timecourse of fluorescence intensity in neurons transfected with scrambled control shRNA (n=25 cells) and CAPS1 shRNA (n=27 cells) compared to untransfected cells (8 cells). (F) Average destaining amplitude at 100 s after start of depolarization for the different conditions as indicated. (G,H) FM1-43 loading and destaining of the readily releasable pool (RRP) of synaptic boutons after CAPS1 knockdown. The RRP and the recycling pool of synaptic boutons were sequentially stained and destained with hypertonic sucrose solution and subsequent elevated K^+ solution according to Pyle and colleagues (2000). (G) Example fluorescence trace of a single synaptic bouton stained with hypertonic sucrose solution and subsequent superfused with elevated K^+ solution. High-K^+-induced destaining of FM1-43-labeled RRP was related to the fluorescence loss from total recycling pool. (H) Histogram of the proportion of RRPs across individual synaptic boutons reveals reduced RRP size. It was mostly synaptic boutons with small RRPs that were affected by CAPS1 knockdown (P=0.01, χ-squared test). Inset: cumulative plot of size of RRP across individual synapses (P<0.001; Kolmogorov–Smirnov test). **P<0.01, ***P<0.001 (one-way ANOVA). Error bars represent s.e.m.

Fusion of BDNF-containing secretory granules is a prerequisite for BDNF release. Consequently, the amount of released BDNF is dependent on the number of fusion events. However, other mechanisms, such as dilation of fusion pores, solubilization of protein aggregates and regulation of kiss-and-run mechanisms after exocytosis could potentially regulate BDNF content release. Therefore, we analyzed CAPS1-dependent release of BDNF from single secretory granules. Neurons were again transfected with CAPS1-shRNA- or control-shRNA-expressing vectors coupled to BDNF–GFP and depolarization-induced (50 mM KCl) release of BDNF was analyzed by monitoring intragranular change of the GFP fluorescence intensity of single secretory granules in dendritic

Journal of Cell Science (2016) 129, 1378-1390 doi:10.1242/jcs.178251

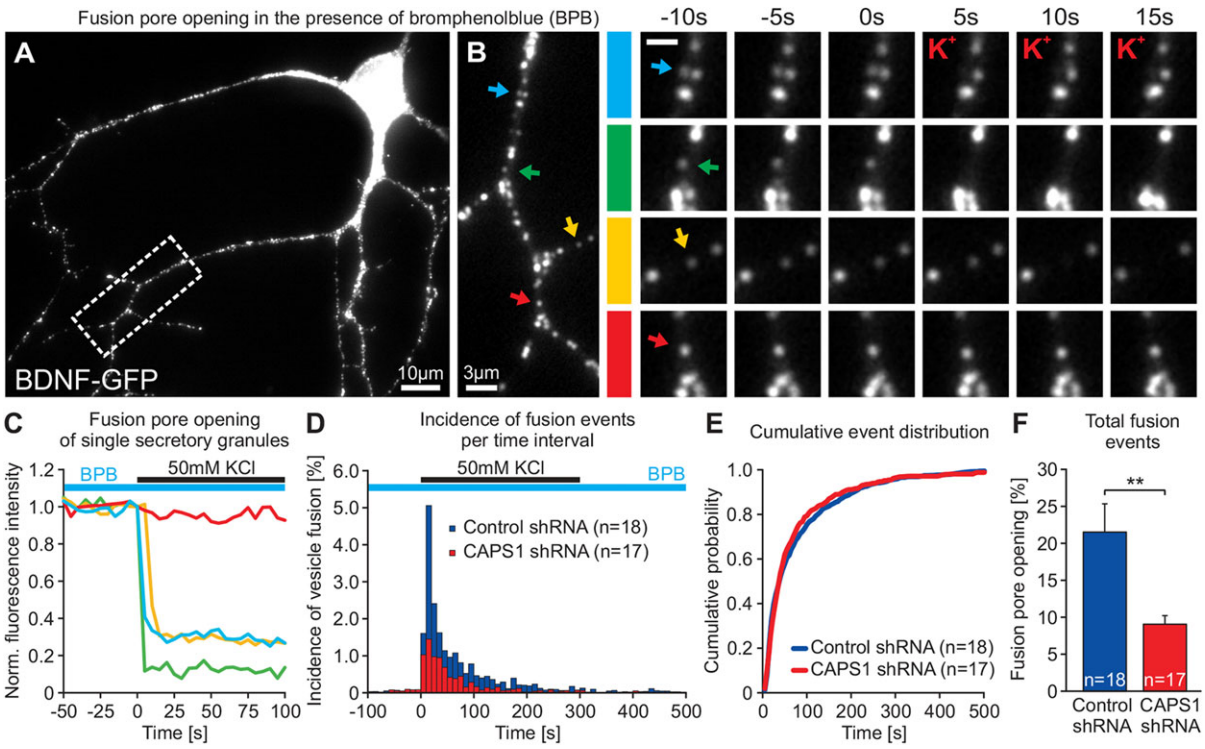

Fig. 2. Reduced number of fusion-competent secretory granules in hippocampal neurons after CAPS1 knockdown. Fusion events of BDNF–GFP-containing vesicles were analyzed by live-cell imaging, monitoring intragranular fluorescence intensity of individual BDNF–GFP vesicles in the presence of the fluorescence quencher Bromophenol Blue (BPB) in control cells (control shRNA) and cells with CAPS1 knockdown (CAPS1 shRNA). (A) Representative picture of a hippocampal neuron showing BDNF–GFP-containing secretory granules. (B) Higher magnification of the dendritic branch shown in boxed area in A. Colored arrows indicate position of four individual BDNF–GFP-containing granules shown at higher magnification in the color-coded picture series on the right (scale bar: 1.5 µm) at different time points of recording. Vesicle fusion was induced by application of 50 mM KCl solution (0 s=start of application). Fusion events were observed as immediate quenching of intragranular GFP fluorescence by extracellular BPB entering the vesicle upon fusion pore opening. (C) Timecourse of fluorescence intensity of the color-coded vesicles marked in B. The red arrow marks a granule that did not show fusion pore opening during the whole measurement. (D) Quantification of vesicle fusion events after CAPS1 knockdown. The number of fusion events was counted in dendritic regions for each time frame and normalized to the total vesicle number of the same region (scrambled control shRNA, 18 cells, 1346 fusion events; CAPS1 shRNA, 17 cells, 542 fusion events). (E) Cumulative probability plot of fusion events displaying no shift in event distribution. (F) Total number of fusion events. Note that this is significantly reduced 500 s after onset of stimulation after knockdown of CAPS1. $^{**}P<0.01$, one-way ANOVA). Error bars represent s.e.m.

branches. First, these measurements were performed in the absence of BPB to avoid quenching of GFP fluorescence. Given that GFP is a pH-sensitive protein showing increased fluorescence intensity at higher pH values (Kneen et al., 1998), we observed for most of the events a transient increase in GFP fluorescence intensity as a consequence of fusion pore opening under these conditions. This increase results from flashing of intravesicular GFP fluorescence by neutralization of the previously acidic granular pH through a fusion pore that is in the process of opening (Fig. 3A, yellow or blue). Another subset of granules showed a sustained loss of fluorescence intensity after a fusion event without a prior fluorescence increase (Fig. 3A, green). In these vesicles, the intragranular pH was already neutral prior to fusion pore opening. Distribution of both events – flashing of intragranular fluorescence versus sustained loss of fluorescence intensity after fusion – was similar under both conditions (percentage of flashing fusion events: scrambled control shRNA, 75.1±6.9%, n=9 cells; CAPS1 shRNA, 70.4± 8.4%, n=8 cells; mean±s.e.m.; P=0.67, one-way ANOVA) (Fig. 3C). To estimate the fraction of released BDNF–GFP per single vesicle after stimulation, we analyzed the average GFP fluorescence intensity over time (Fig. 3D). As is evident from the figure, initial fluorescence increase and subsequent decay of GFP fluorescence were rather slow under these conditions because fusion pore opening of different vesicles was not synchronized to the start of depolarization but occurred with a delay of up to 100 s between different vesicles (see also Fig. 2D). Consequently, an increase in the mean fluorescence intensity became apparent after a slight delay of 10–30 s after the start of depolarization (Fig. 3D). At later time points, different vesicular events were superimposed. Some granules showed increased GFP fluorescence intensity due to intragranular neutralization after fusion events. Other granules displayed loss of fluorescence intensity resulting from release of BDNF–GFP. Both types of processes overlapped in time and the respective fluorescence changes interfered in the average trace over all vesicles (Fig. 3D). As a consequence, no discrete peak in fluorescence intensity was evident but rather a plateau was reached that declined after most of the fusion events had occurred. To estimate the average BDNF–GFP content release from each single secretory granule, the fluorescence traces of all individual vesicles were aligned such that the time point of fusion was set to 0 s. The resulting aligned fluorescence trace is shown in Fig. 3E and is an estimate of intragranular pH-dependent increase in GFP fluorescence intensity and the average fraction of BDNF released from single granules. First, we analyzed the increase in fluorescence intensity following the fusion events. For this quantification, fluorescence intensity of each single secretory granule before fusion (time point=0) was set to 100% and peak fluorescence after fusion was analyzed. Here, we observed a

Journal of Cell Science (2016) 129, 1378-1390 doi:10.1242/jcs.178251

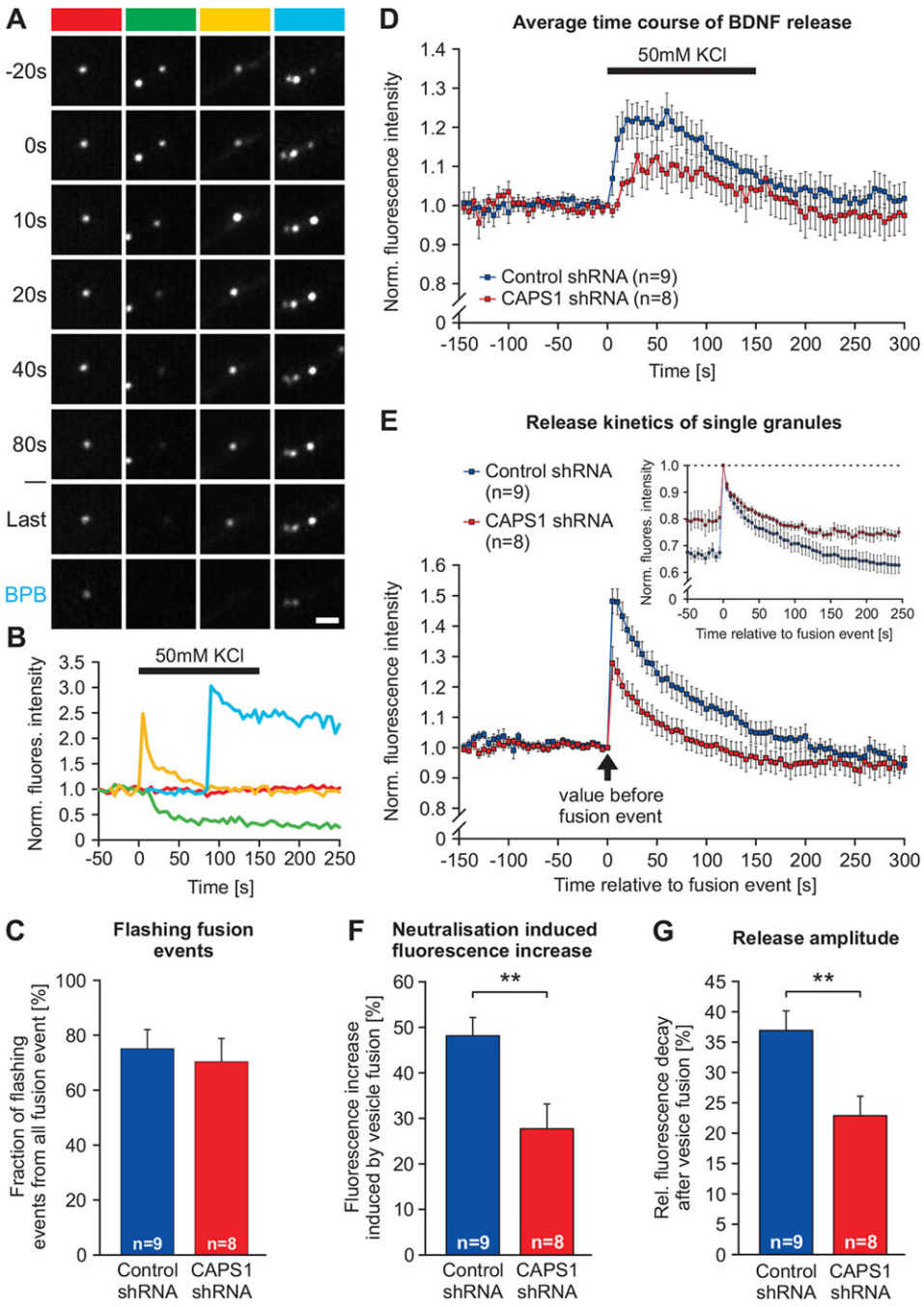

Fig. 3. Reduction of BDNF content release from secretory granules after CAPS1 knockdown as measured in the absence of BPB. BDNF content release was analyzed by live-cell imaging, monitoring intragranular change in the GFP fluorescence intensity of single secretory granules in dendritic branches in control cells (control shRNA) and cells with CAPS1 knockdown (CAPS1 shRNA). (A) Different secretory granules (green, yellow and blue) showing fusion events as indicated by the change in fluorescence intensity in the absence of BPB at different time points compared to a secretory granule showing no fusion pore opening (red). For most of the fusion events, BDNF–GFP fluorescence increased due to the neutralization of the intragranular pH after exocytosis. Content release was observed as fluorescence decay after the neutralization step. At the end of the release measurement, neurons were superfused with BPB (0.3 mM) to differentiate between vesicles in an open or closed state at this time point. Scale bar: 2 µm. (B) Timecourse of fluorescence intensity of BDNF–GFP-containing secretory granules shown in A. (C) 'Flashing' events such as those shown in B were present to a similar extent in CAPS1-knockdown cells to in control cells. (D) Average timecourse of decay in fluorescence intensity during secretory granule release. Time point 0 indicates the start of depolarization. Note that the timecourse of the initial fluorescence increase and the subsequent decay were rather slow. (E) Aligned average timecourse of decay in fluorescence intensity from single secretory granules after fusion pore opening from the same ROIs analyzed in D (scrambled control shRNA: 9 cells, 110 events; CAPS1 shRNA: 8 cells, 57 events). All single vesicle events analyzed here are normalized to the time point immediately before vesicle fusion (t=0 s). Inset, average fluorescence decay from single secretory granules. Here, the peak fluorescence of individual vesicle was set to 100% (at t=0 s) to quantify the release amplitude (i.e. decrease in fluorescence intensity due to release). (F) Quantification of the initial fluorescence increase after fusion pore opening in single BDNF–GFP-containing secretory granules (see E). The initial fluorescence increase was significantly reduced in secretory granules after CAPS1 knockdown. (G) Quantification of the fluorescence decay after fusion pore opening and resulting pH neutralization of the vesicles (see E, inset). The maximal fluorescence intensity was set to 100% and the remaining fluorescence intensity 300 s after fusion pore opening was analyzed. Content release estimated as relative fluorescence decrease after fusion pore opening was significantly reduced after CAPS1 knockdown. $^{**}P$<0.01 (one-way ANOVA). Error bars represent s.e.m.

Journal of Cell Science (2016) 129, 1378-1390 doi:10.1242/jcs.178251

smaller peak fluorescence intensity (reflecting the pH-dependent increase in GFP fluorescence intensity) in secretory granules of neurons transfected with CAPS1 shRNA as compared to control (Fig. 3E,F: control shRNA, 48.2±4.0%, n=9 cells; CAPS1 shRNA, 27.7±5.4%; n=8 cells; mean±s.e.m.; P<0.01, one-way ANOVA). To estimate the average fraction of BDNF–GFP that was released from single granules, the maximum fluorescence intensity of each single secretory granule after fusion (Fig. 3E, inset: time point=0) was set to 100% and the relative fluorescence decay 300 s after fusion (i.e. the release amplitude) was analyzed (Fig. 3E, inset, and 3G). Interestingly, the release amplitude was significantly reduced following CAPS1 knockdown (Fig. 3G, control shRNA, 36.9±3.2%, n=9 cells; CAPS1 shRNA, 22.9±3.2%; n=8 cells; mean±s.e.m.; P<0.01, one-way ANOVA). This effect could not be explained by CAPS1-induced changes in synaptic transmission, as BDNF–GFP release measurements in the presence of synaptic blockers revealed the same results (Fig. S3G,H). A similar reduction in BDNF–GFP release amplitude was obtained in hippocampal neurons transfected with small interfering RNA (siRNA) directed against CAPS1 (Fig. S3I,J), indicating that the effect was most likely not due to overload of the cellular microRNA machinery by overexpression of CAPS1 shRNA. To judge the release amplitude per single vesicle correctly, it is necessary to prove that all vesicles undergoing fusion are still open at the end of the experiment. This was verified by superfusion of neurons with BPB at the end of each release measurement to quench all vesicular GFP fluorescence that was still accessible from the extracellular side. This procedure allowed us to specifically investigate BDNF-containing granules that did not undergo reclosure and reacidification so that intragranular decrease of GFP fluorescence intensity could be attributed clearly to released BDNF from these secretory granules. In contrast, non-fusing BDNF-GFP vesicles in the same field of view that had no access to the extracellular solution showed dimming of GFP fluorescence after BPB superfusion (Fig. 3A, red). This dimming of GFP fluorescence resulted from absorption of light in the light path by BPB rather than from quenching of the green photons emitted by GFP, which is only observed if BPB is in very close proximity to GFP. These two phenomena could be clearly distinguished in our culture (Fig. S2G–I). Analysis of opening states of BDNF-containing granules by superfusion of neurons with BPB at the end of the release measurements revealed that all vesicles undergoing stimulation-induced release (flashing) were still open at the end of the measurement. Whether these BDNF puncta represent BDNF–GFP-containing deposits or granules with an open fusion pore cannot be distinguished with this technique. To test whether our BPB quenching approach in fact detects stimulation-induced fusion of previously closed BDNF–GFP vesicles or rather quenches BDNF–GFP deposits or open granules that were present long before the start of stimulation, we superfused BDNF–GFP-transfected cells with BPB and analyzed the fraction of quenched BDNF–GFP-containing granules in the absence of stimulation. These data revealed a low abundance of these BDNF–GFP puncta with access to the extracellular space before stimulation, both, after CAPS1 knockdown as well as under control conditions (Fig. S2I, control shRNA, 0.54±0.39%, n=3 cells; CAPS1 shRNA, 0.66±0.66%; n=3 cells; mean±s.e.m.; P=0.88, one-way ANOVA). Taken together, these results reveal an effect of CAPS1 protein on the extent of depolarization-induced BDNF release from single secretory granules. Furthermore, these results suggest a role for CAPS1 in regulating the intragranular pH value of BDNF vesicles before the fusion event takes place.

Knockdown of CAPS1 leads to an impairment of intragranular acidification

GFP is a pH-sensitive protein. As shown in the last paragraph, the fluorescence intensity of GFP is reduced by acidic pH. Accordingly, the increase in GFP fluorescence intensity after fusion pore opening is a read-out of the intragranular neutralization following the exocytotic event. Thus, the more acidic the pH value in the granule before the fusion event, the larger is the fluorescence increase upon fusion. To determine the reason for the reduced increase in GFP fluorescence intensity upon fusion pore opening after CAPS1 knockdown (Fig. 3F) in more detail, we analyzed the pH value as well as the BDNF–GFP content of single vesicles. To estimate whether the BDNF–GFP content of single secretory granules was influenced after CAPS1 knockdown, we superfused transfected neurons with solution containing 50 mM NH_4Cl to adjust the intracellular as well as intragranular pH value to the same level (Fig. S4A–F). NH_4Cl dissociates into NH_4^+ and Cl^-, which is in equilibrium with NH_3 and H^+. NH_3 then rapidly diffuses across the cell membrane and neutralizes the intracellular and intragranular pH (Boron and De Weer, 1976). The fluorescence increase and the absolute value of GFP fluorescence during NH_4Cl superfusion were quantified for single secretory granules (Fig. S4E,F). This analysis revealed that the NH_4Cl induced fluorescence increase of all vesicles was significantly reduced in CAPS1-shRNA-transfected neurons, indicating a less-acidic intragranular pH in these vesicles under control conditions. Although the absolute fluorescence intensity of individual granules showed high variations before NH_4Cl application for both conditions, the absolute intragranular fluorescence intensity during NH_4Cl perfusion was similar (Fig. S4F). These results indicate a comparable loading of secretory granules with BDNF–GFP under control conditions and following CAPS1 knockdown. A similar CAPS1-knockdown-induced neutralization was observed for synaptic vesicles that were probed for pH using synapto-pHluorin. In addition, synaptic vesicles showed a reduced increase in fluorescence intensity and comparable absolute intravesicular fluorescence intensity after NH_4Cl perfusion in CAPS1-shRNA-transfected neurons, indicating a less-acidic intravesicular pH after CAPS1 knockdown (Fig. S4G–K).

We next aimed to determine the exact pH value of the BDNF-containing vesicles before the fusion event. Therefore, we measured the intragranular pH of BDNF vesicles using GFP as an intrinsic pH indicator according to Kneen and colleagues (Kneen et al., 1998). shRNA-transfected hippocampal neurons were initially superfused with control buffer (pH 7.4) followed by sequential superfusion with pH-calibrated solutions containing the H^+/K^+ antiporter nigericin as well as the K^+ ionophore valinomycin at distinct pH values (Fig. 4A,B). The ionophores caused pH equilibration between the extracellular space and the cytosol as well as the granule lumen. Intragranular GFP fluorescence was measured by time-lapse video microscopy during superfusion with the different solutions with defined pH (Fig. 4E). A calibration curve for each individual vesicle was plotted, thus allowing us to interpolate the initial pH value of single vesicles at the start of the experiment (Fig. 4F). Although the pH value of single BDNF-containing vesicles under control conditions approached 5.80±0.03 (n=6 cells), this value was significantly increased to 6.73±0.10 after knockdown of CAPS1 protein (n=6 cells, mean±s.e.m.; P<0.001, one-way ANOVA) (Fig. 4G). To determine whether the change in intragranular pH was simply due to an overall change in intracellular pH after CAPS1 knockdown, we transfected hippocampal neurons with GFP plasmids and analyzed the

Journal of Cell Science (2016) 129, 1378-1390 doi:10.1242/jcs.178251

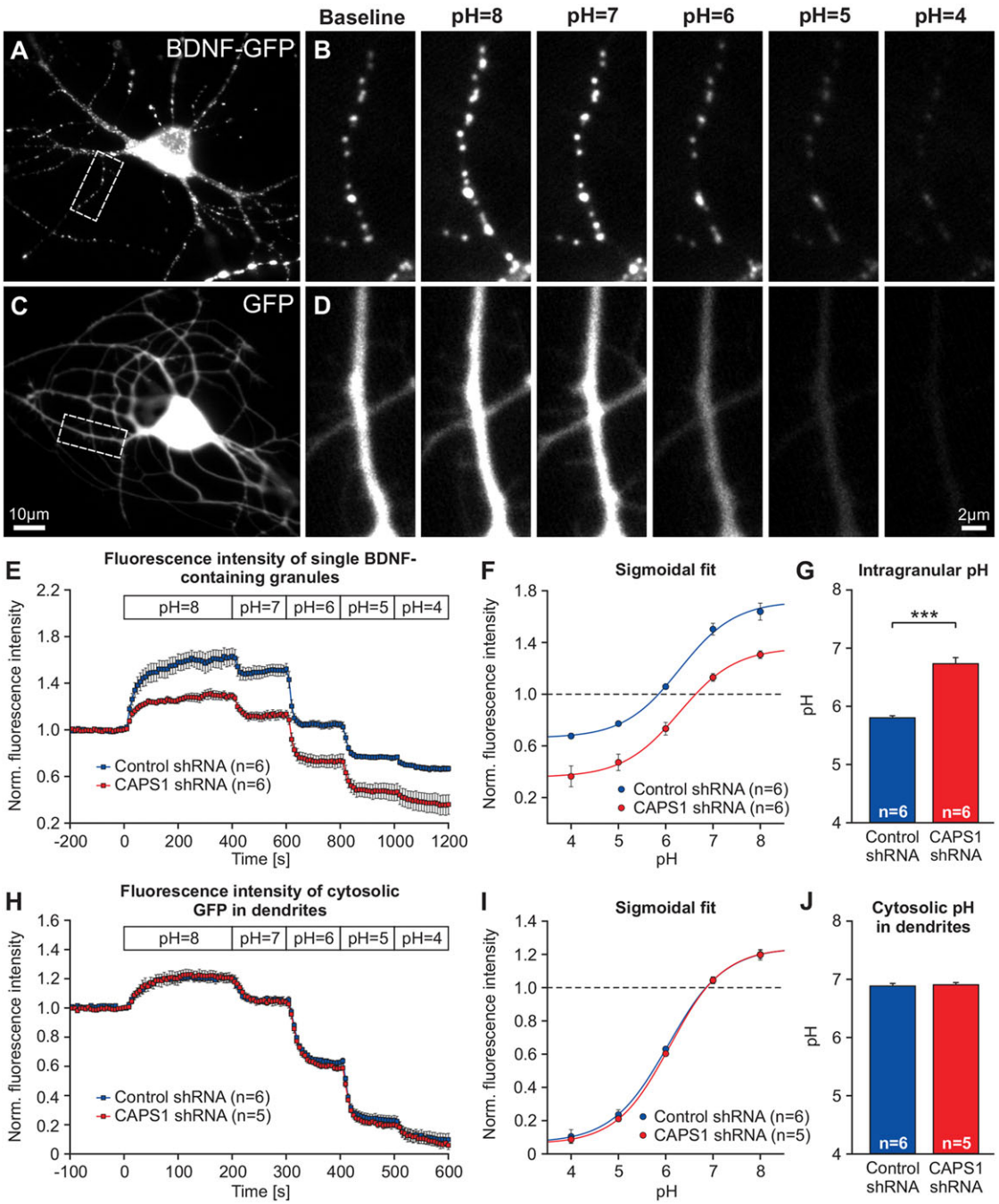

Fig. 4. Increase in intragranular pH value after knockdown of CAPS1 protein. Intragranular pH of BDNF-containing vesicles was measured by using GFP as an intrinsic pH indicator in control cells (control shRNA) and cells with CAPS1 knockdown (CAPS1 shRNA). (A–D) Hippocampal neurons transfected with BDNF–GFP (A) or GFP (C), respectively, were initially superfused with control buffer (pH=7.4) for 200 s to measure baseline fluorescence intensity. (B,D) After baseline recording, neurons were superfused with calibration solutions containing nigericin and valinomycin at different pH values until a plateau of fluorescence intensity was reached. Boxed areas show the fluorescence intensity of dendritic regions at the indicated pH values at higher magnification. (E) Average intragranular fluorescence intensity of single BDNF–GFP-containing secretory granules during pH titration normalized to baseline fluorescence intensities (scrambled control shRNA: 6 cells, 59 vesicles; CAPS1 shRNA: 6 cells, 57 vesicles). Fluorescence intensities at different pH were used to interpolate intragranular pH. (F) Average calibration curve for single secretory granules. Sigmoidal fitting of the data was used to calculate the pH value of single granules at the start of the experiment (−200–0 s). (G) Quantification of intragranular pH. Note the strong increase of pH of single BDNF-containing vesicles in neurons transfected with CAPS1 shRNA. (H–J) Hippocampal neurons expressing GFP in dendrites were analyzed similarly to as shown in E–G. Cytosolic pH value was calculated in dendritic branches (scrambled control shRNA, 6 cells, 44 regions; CAPS1 shRNA, 5 cells, 35 regions) of hippocampal neurons. Note that the pH value of intracellular cytosolic compartments was similar for both conditions ***P<0.001 (one-way ANOVA). Error bars represent s.e.m.

cytoplasmic pH value after CAPS1 knockdown (Fig. 4H–J). Again, cells were initially superfused with control buffer at pH 7.4 followed by superfusion with calibration solutions as described above (Fig. 4C,D). Cytoplasmic GFP fluorescence was measured by time-lapse video microscopy in dendritic branches of hippocampal neurons similar to those used for secretory granule recordings (Fig. 4H). A calibration curve for dendritic branches (Fig. 4I) was plotted and the initial pH value of cytosolic compartments at the

Journal of Cell Science (2016) 129, 1378-1390 doi:10.1242/jcs.178251

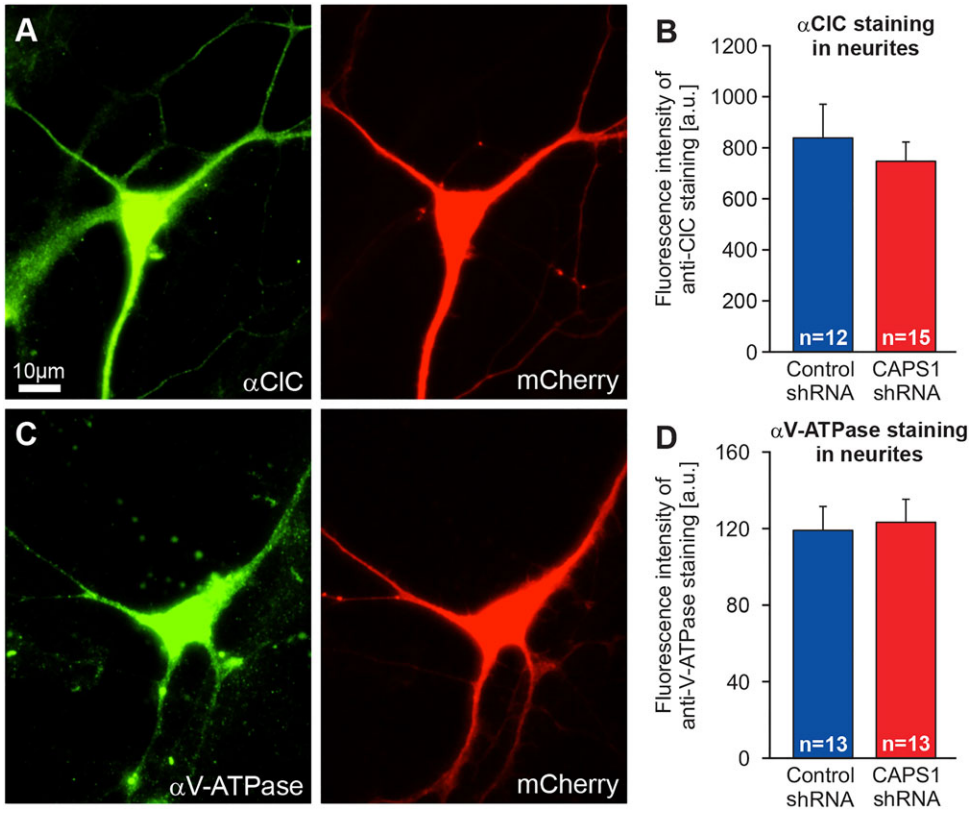

Fig. 5. Expression of V-type ATPase and ClC-3 are unaffected by CAPS1 shRNA. (A) Representative image of a hippocampal neuron transfected with control shRNA plasmid coexpressing mCherry (red) immunostained with an antibody directed against endogenous granular chloride channel (αClC, green). (B) Quantification of dendritic ClC immunofluorescence in control cells (control shRNA) and cells with CAPS1 knockdown (CAPS1 shRNA). Note the apparently unchanged ClC expression after CAPS1 knockdown (P>0.05, one-way ANOVA). (C) Representative image showing a hippocampal neuron transfected with control shRNA plasmid coexpressing mCherry (red) immunostained with an antibody directed against endogenous V-ATPase protein (green). (D) Quantification of dendritic V-ATPase immunofluorescence. Note the apparently unchanged V-ATPase after CAPS1 knockdown (P>0.05, one-way ANOVA). Error bars represent s.e.m.

start of the experiment was interpolated (Fig. 4J). The pH value of dendritic regions (control shRNA, 6.89±0.04, n=6 cells; CAPS1 shRNA, 6.91±0.04, n=6 cells; mean±s.e.m.; P=0.74, one-way ANOVA) was similar in hippocampal neurons transfected with CAPS1 shRNA compared to control. Interestingly, these results suggest a specific increase of intragranular pH value after knockdown of CAPS1 protein.

Acidification is an important step during maturation of secretory granules. The highly conserved multimeric protein complex of the vacuolar-type H^+-ATPase (V-ATPase) is known to establish and maintain the luminal pH gradient (Wu et al., 2001). Furthermore, the granular chloride channels (ClCs) have been described previously to contribute to the acidification of secretory granules (Deriy et al., 2009). To test whether shRNA-mediated knockdown of CAPS1 decreased the expression levels of these proteins, we checked expression levels of the V-ATPase as well as the ClCs after CAPS1 knockdown. Immunocytochemical stainings with antibodies directed against V-ATPase and ClCs revealed a similar immunofluorescence, suggesting unchanged expression of V-ATPase and ClCs under both conditions (Fig. 5). To address whether the CAPS1-knockdown-dependent altered properties of fusion and BDNF release (compare Figs 2 and 3) were a consequence of the intragranular pH changes (compare Fig. 4 and Fig. S4), we repeated the analysis of fusion events as well as of BDNF content release under conditions of equal intragranular pH for both sets of cells. Therefore, hippocampal neurons were preincubated with the proton pump inhibitor bafilomycin (1 µM) for 30 min before recordings. Owing to the leakage of protons from secretory granules into the cytoplasm and the inhibited re-acidification of vesicles in the presence of bafilomycin, the intragranular pH was neutralized under these conditions. Depolarization-induced vesicle fusion events were measured in the presence of 0.3 mM BPB and bafilomycin, and were detected as loss of intragranular fluorescence intensity resulting from immediate quenching of intragranular GFP fluorescence upon entrance of BPB. Again, the number of fusion events per time interval and the number of fusion events were significantly reduced after CAPS1 knockdown (Fig. 6A,B, control shRNA, 22.9±3.3%, n=6 cells; CAPS1 shRNA, 7.5±1.7%; n=6 cells; mean±s.e.m.; P<0.01, one-way ANOVA). The rate of fusion events was similar to the rate of fusion events under physiological pH conditions (compare Fig. 2F,H). Taken together, these results suggest that the intragranular pH effect following CAPS1 knockdown is not responsible for the CAPS1-knockdown-induced decrease in the number of fusion-competent secretory granules.

In addition to fusion of BDNF vesicles, we also determined the effect of CAPS1 knockdown on content release of BDNF in the presence of 1 µM bafilomycin to inhibit the V-ATPase. These release experiments were performed in the absence of BPB. Owing to the neutralization of intragranular pH by inhibiting re-acidification of vesicles in the presence of bafilomycin, a fusion pore opening-induced increase in GFP fluorescence intensity was not observed, and the timecourse of fluorescence intensity was characterized by a loss of intragranular fluorescence intensity after vesicle fusion (Fig. 6C). Again, the release amplitude at 300 s after stimulation was significantly reduced by knockdown of CAPS1 (Fig. 6D,F, control shRNA, 42.4±2.1%, n=6 cells; CAPS1 shRNA, 21.4±3.9%; n=6 cells; mean±s.e.m.; P<0.001, one-way ANOVA). Similar results were obtained after adjustment of intragranular pH with NH_4Cl (Fig. 6E–H). These data indicate that neither intragranular pH before induction of fusion nor inhibition of V-ATPase in itself are responsible for the reduced BDNF content release observed following acute CAPS1 knockdown. This suggests that the effects of CAPS1 knockdown on fusion events and content release did not result from the additional intragranular pH change that was observed in parallel in these experiments.

Journal of Cell Science (2016) 129, 1378-1390 doi:10.1242/jcs.178251

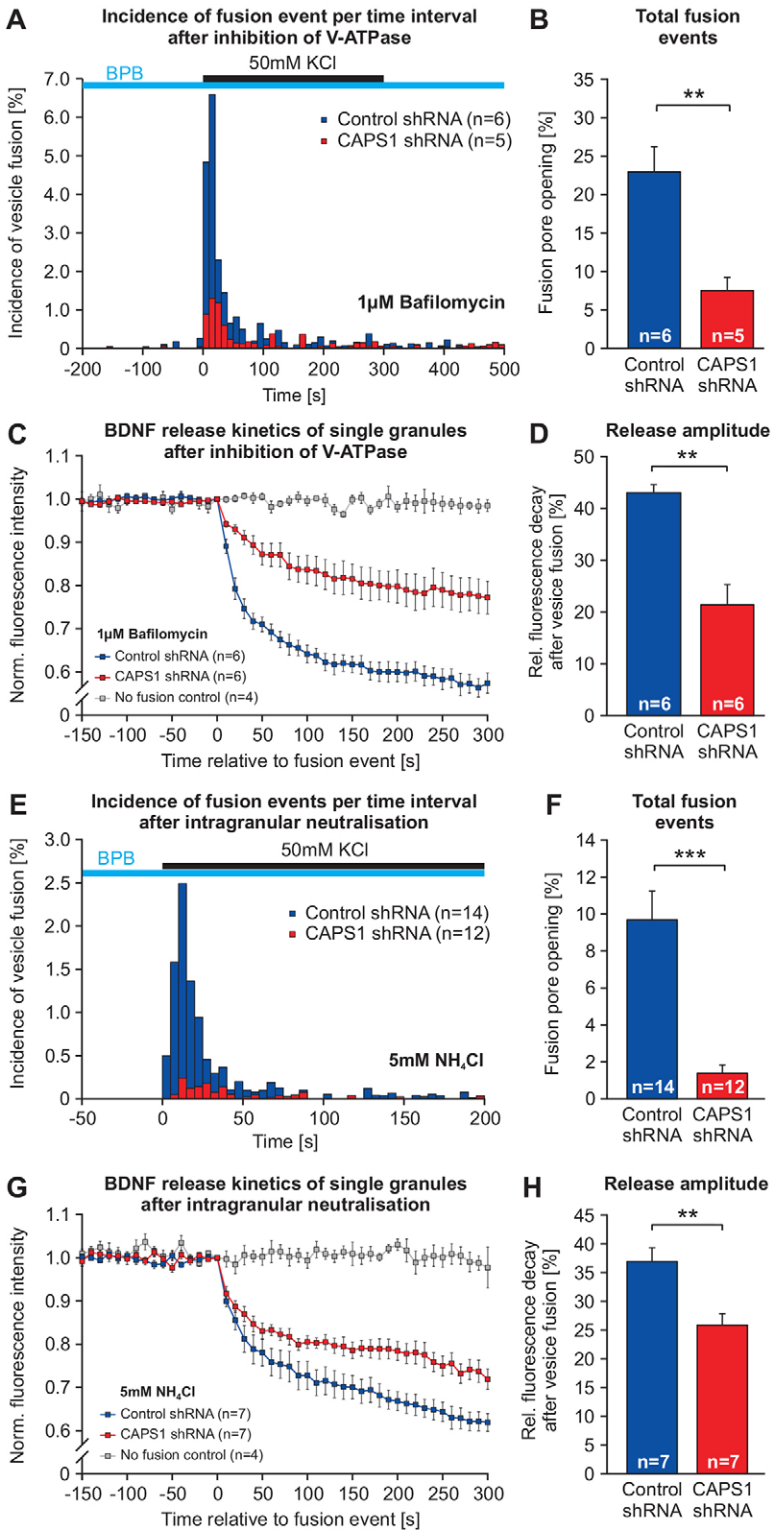

Fig. 6. CAPS1 function in prefusion steps and BDNF content release was not affected by intragranular pH. (A–D) Fusion events and BDNF content release were analyzed (as shown in Figs 2 and 3) after inhibiting V-ATPase with bafilomycin and thereby adjusting intragranular pH to the same level under control conditions and after acute CAPS1 knockdown. (A) Quantification of vesicle fusion events with the BPB imaging method after CAPS1 knockdown in the presence of bafilomycin. Fusion events were observed as immediate quenching of intragranular GFP fluorescence by extracellular BPB upon fusion pore opening. Rate of fusion events was determined for each time frame (scrambled control shRNA, 6 cells, 340 fusion events; CAPS1 shRNA, 5 cells, 113 fusion events) and normalized to the total number of granules in the dendritic stretch. (B) The proportion of dendritic vesicles showing fusion pore opening until 500 s after onset of stimulation was strongly reduced after CAPS1 knockdown. (C,D) BDNF release was analyzed after inhibiting V-ATPase with bafilomycin. (C) Average timecourse of relative GFP fluorescence intensity of single secretory granules from neurons transfected either with control shRNA (n=6 cells, 61 events) or CAPS1 shRNA (n=6 cells, 44 events). Note that the reduced release amplitude (i.e. decrease in fluorescence intensity due to release) upon CAPS1 knockdown was still present after adjustment of intragranular pH with bafilomycin. (D) Average amplitude of fluorescence decay at 300 s after the onset of vesicle fusion. (E–H) Fusion events and BDNF content release were analyzed for both conditions after adjustment of intragranular pH to a similar level with NH_4Cl. Incidence of fusion events (E), total number of fusion events (F), BDNF release kinetics (G) as well as BDNF release amplitude (H) after adjustment of intragranular pH with NH_4Cl were similarly affected by CAPS1 knockdown as observed without prior pH adjustment. **P<0.01, ***P<0.001 (one-way ANOVA). Error bars represent s.e.m.

DISCUSSION

The cytosolic protein CAPS1 is known to regulate dense core vesicle (DCV) exocytosis in neuroendocrine cells, although its exact function during the secretion process remains controversial (Sugita, 2008). Here, we analyzed the role of CAPS1 in synaptic vesicle exocytosis and dendritic BDNF release after acute knockdown of CAPS1 protein. Combining live-cell imaging of fluorescently labeled vesicles and shRNA-mediated gene silencing, we show that acute knockdown of CAPS1 decreased the efficiency of synaptic vesicle release as well as secretory granule maturation and exocytosis in primary hippocampal neurons. Our results demonstrate, for the first time, that CAPS1 has a previously unrecognized function in regulating the intragranular pH of secretory granules. Furthermore, our results show that acute single-cell knockdown of CAPS1, with the vast majority of neurons in the network still expressing CAPS1, strongly reduced

Journal of Cell Science (2016) 129, 1378-1390 doi:10.1242/jcs.178251

the number of fusion-competent secretory granules in dendrites of CAPS1-depleted hippocampal neurons. Moreover, CAPS1 knockdown significantly lowered the fraction of BDNF released per single secretory granule. Importantly, these effects of CAPS1 knockdown on fusion events and BDNF-content release occurred independently of the change in intragranular pH following CAPS1 knockdown, which was shifted to a more neutral pH before fusion.

CAPS1 was initially described to affect Ca^{2+}-dependent monoamine release from DCVs in permeabilized PC12 cells (Walent et al., 1992). Additionally, electrophysiological recordings in constitutive CAPS1-knockout mice have revealed that CAPS1 is an important protein for the generation of readily releasable synaptic vesicles (Jockusch et al., 2007). Our results strengthen these findings that CAPS1 is important for neurotransmitter release from synaptic vesicles in neurons, even under conditions of acute and incomplete knockdown of the protein (Fig. 1). Using FM1-43 staining methods, our results reveal that the number of active presynaptic terminals remained unchanged after transient knockdown of CAPS1 protein (Fig. S1). However, the size of the RRP and the recycling pool, as characterized by staining and destaining amplitude of single FM-loaded synaptic boutons, were significantly reduced, confirming that CAPS1 also has a role of in neurotransmitter release from synaptic vesicles in conditions of acute knockdown (Fig. 1G,H; Fig. S1I,J). These results are in line with the reduction of the RRP size to 42% of wild-type levels in constitutive CAPS1-knockout mice (Jockusch et al., 2007). Furthermore, our results indicate a CAPS1-induced increase in synaptic vesicle pH (Fig. S4G–K), suggesting reduced pH-dependent neurotransmitter loading of synaptic vesicles. This effect could account for the previously described drastic reduction in evoked excitatory post-synaptic current (EPSC) amplitudes in constitutive CAPS1-knockout mice (Jockusch et al., 2007).

Importantly, our data demonstrate a role of CAPS1 knockdown on distinctly different steps in the life cycle of secretory granules in hippocampal neurons. Thus, our results show that CAPS1 acts at several stages of secretory granule maturation and exocytosis. First, knockdown of CAPS1 led to impaired intragranular acidification (Fig. 4; Fig. S4). Second, the number of single-vesicle fusion pore events in hippocampal neurons was reduced to ∼50% after acute CAPS1 knockdown (Fig. 2). Finally, the fraction of BDNF which is released from single secretory granules was significantly reduced (Fig. 3). Notably, altered fusion pore opening and reduced BDNF release from single secretory granules after transient CAPS knockdown both occurred independently of the altered intragranular pH (Fig. 6).

The observed significant increase in intragranular pH after CAPS1 knockdown reveals a new and previously unrecognized function of CAPS1 in secretory granule acidification (Fig. 4; Fig. S4). The shift of intragranular pH before fusion to less-acidic values upon CAPS1 knockdown (i.e. from 5.8 to 6.7) was not accompanied by a respective change in cytosolic pH (Fig. 4). Acidification is an important step during maturation of secretory granules. The highly conserved multimeric protein complex of the vacuolar-type H^+-ATPase (V-ATPase) is known to establish and maintain the luminal pH gradient relative to the cytoplasm (Wu et al., 2001). The reduction of luminal acidification upon knockdown of endogenous CAPS1 protein that we discovered here suggests a protein–protein interaction between CAPS1 and the V-ATPase. However, granular ClCs are also known to contribute to the acidification of secretory granules by a mechanism involving shunting of currents through proton pumps and increasing the intravesicular chloride concentration (Deriy et al., 2009). Whether direct molecular association of CAPS1 with one of these two proteins (i.e. V-ATPase or ClCs) might account for the increased intragranular pH after knockdown of CAPS1 protein remains to be determined. Given that intravesicular acidification drives the efficacy of vesicular monoamine transporters (Henry et al., 1994), the changed intragranular pH that we observed might explain the described CAPS1-induced deficits in monoamine vesicle loading in neuroendocrine cells (Brunk et al., 2009; Speidel et al., 2005; Südhof, 2005). However, although in our experiments the intragranular pH was increased in hippocampal neurons with reduced CAPS1 expression, the BDNF content of secretory granules was unchanged (Fig. S4F). These findings, together with the unchanged density of BDNF granules in hippocampal neurons (Fig. S2D,E), indicate that there are no major deficits in protein packing or processing of secretory granules after CAPS1 knockdown. With respect to BDNF packaging, this was an expected finding because BDNF loading into secretory granules is not driven by intragranular pH. Furthermore, the data are in line with electron microscopy studies showing no abnormalities in the number or distribution of DCVs in neuroendocrine and neuronal cells (Fujita et al., 2007; Jockusch et al., 2007; Speidel et al., 2005). However, in cells obtained from adult tissue of constitutive CAPS1-knockout mice, the distance of DCVs to the plasma membrane in neuroendocrine cells (Speidel et al., 2005), as well as the density of presynaptic DCVs in hippocampal CA3 neurons (Sadakata et al., 2013) is altered, which might be due to secondary effects caused by a developmental problem in these constitutive knockout mice.

Our results also reveal that the number of fusion events of BDNF-containing vesicles was reduced by 50% after acute CAPS1 knockdown in hippocampal neurons (Fig. 2). These findings obtained after acute single-cell knockdown of CAPS1 to roughly 35% of WT protein levels are in line with previous observations indicating a function of CAPS1 in regulating prefusion events of DCVs in neuroendocrine cells (Ann et al., 1997; Grishanin et al., 2004; Hay and Martin, 1992; Sugita, 2008; Walent et al., 1992). Importantly, the reduced vesicle fusion rate after acute CAPS1 knockdown occurred independently of changes in intragranular pH, suggesting distinct mechanisms of action of CAPS1 for both processes. Recent studies have suggested a role for CAPS2, which represents another CAPS protein isoform, in the release of BDNF from hippocampal neurons (Sadakata et al., 2014; Shinoda et al., 2011). The expression of CAPS2 has been described to be complementary to the expression of CAPS1 in hippocampal neurons (Sadakata et al., 2006). Just as for CAPS1, also the knockout of CAPS2 has been shown to reduce the number of fusion events in BDNF-containing granules (Shinoda et al., 2011). This suggests that either of the two CAPS isoforms, which are usually not co-expressed in individual neurons (Sadakata et al., 2006), can regulate BDNF vesicle exocytosis.

The size of fusion pores is important for the efficiency of activity-dependent content release from secretory granules. Given that BDNF secretory granules of hippocampal neurons contain a cocktail of additional small molecules and proteins (Brigadski and Lessmann, 2014), the size and the duration of fusion pore opening additionally influence BDNF content release. In previous studies, the role of CAPS1 was mostly analyzed for monoamine release (Ann et al., 1997; Hay and Martin, 1992; Walent et al., 1992) or neuropeptide secretion from DCVs in neuroendocrine cells (Fujita et al., 2007). In our study, we show that CAPS1 also regulates secretion of the protein BDNF–GFP in central hippocampal neurons (Figs 2 and 3), which has a molecular weight of 40 kDa. These results suggest a possible function of

Journal of Cell Science (2016) 129, 1378-1390 doi:10.1242/jcs.178251

CAPS1 not only during the prefusion steps of DCV secretion but also for postfusion events, such as dilation of fusion pores, solubilization of protein aggregates and possibly also regulation of kiss-and-run mechanisms after exocytosis. Given that BDNF–GFP content release was analyzed in vesicles that were still open at the end of measurements, we could rule out that reduced BDNF content release after CAPS1 knockdown was due to a shorter overall opening time of fusion pores. Deficits in the incidence of fusion pore openings or BDNF content release after CAPS1 knockdown could potentially result indirectly from the CAPS1-knockdown-induced change in intragranular pH. However, we observed the same alterations in fusion events and content release of BDNF–GFP vesicles after inhibiting the V-ATPase by bafilomycin, thereby adjusting intragranular pH prior to release to the same level under both conditions (i.e. CAPS1 knockdown and control). These results suggest that there is not a causal connection between intravesicular pH regulation by CAPS1 before fusion of secretory granules and the CAPS1-dependent effects on later steps of secretory granule exocytosis.

Activity-dependent release of BDNF is assumed to be a key element for the induction and expression of synaptic plasticity (Edelmann et al., 2014). Thus, CAPS1-induced changes in BDNF release could affect long-term potentiation (LTP) in neurons. Given that fusion events of secretory granules and BDNF content release are controlled by CAPS1, regulatory elements of CAPS1 function might influence BDNF release and therefore LTP processes. To date, little is known about the regulation of CAPS1 protein expression. In neuroendocrine cells, CAPS1 interacts, through its pleckstrin homology domain, with the plasma membrane during Ca^{2+}-dependent exocytosis (Ann et al., 1997). In this process, CAPS1 functions as a phosphatidylinositol bisphosphate (PIP_2)-binding protein (Grishanin et al., 2004). Thus, mechanisms leading to a change in the PIP_2 pool, like hydrolysis of PIP_2 by phospholipases or synthesis of PIP_2 are possible candidates to fine-tune BDNF-release-dependent plasticity processes.

In the present study, we show that CAPS1 protein plays an important role during protein release from secretory granules in hippocampal neurons. The cytosolic protein CAPS1 regulates several stages of secretory granule processing. Specifically, intragranular pH was increased, and the number of fusion events, as well as the absolute amount of protein released from individual vesicles in hippocampal neurons, was significantly decreased after acute knockdown of CAPS1 protein. Therefore, fine-tuning of CAPS1 function represents a potential regulatory mechanism to adjust BDNF release during activity-dependent synaptic plasticity processes.

MATERIALS AND METHODS

Reagents

Arabinofuranosyl cytidine (AraC), Bromophenol Blue, $CaCl_2$, glucose, glycine, KCl, NH_4Cl and valinomycin were from Sigma; B27 supplement, 6,7-dinitroquinoxaline-2,3-dione (DNQX) and DL-2-amino-5-phosphonopentanoic acid (DL-AP5) were from Tocris Bioscience; Bafilomycin A1 was from Merck Chemicals; basal medium Eagle (BME), fetal calf serum (FCS), neurobasal (NB) medium, nigericin and PBS were from Life Technologies; pEGFP-N1 was from CloneTech.

Hippocampal microcultures

All experiments were performed in accordance with the ethical guidelines for use of animals in experiments and were approved by the local animal care committee (Landesverwaltungsamt Sachsen-Anhalt).

Microcultures were prepared as described previously (Lessmann and Heumann, 1998). Primary cortical astrocytes from P0–P3 Sprague–Dawley rats were isolated and cultured for 2–3 weeks in BME medium supplied with 10% FCS. After confluence was reached, astrocytes were seeded on glass coverslips at a density of 50,000 cells per 3.5-cm culture dish. At 3 days *in vitro* (DIV), proliferation was inhibited by adding 3–5 µM AraC to the medium. After 2–3 weeks, hippocampal neurons of C57BL/6 mice were isolated from P0–P2 mice and seeded onto the astrocyte islands. Neurons were allowed to attach to astrocytes before the culture medium was replaced by neurobasal medium containing 2% B27 supplement.

Transfection

Hippocampal neurons were transfected at 6–8 DIV with the respective plasmids by using the Ca^{2+} phosphate precipitation method (Haubensak et al., 1998). In brief, up to 4.5 µg plasmid DNA per 3.5 cm culture dish was used to form precipitates in the presence of 10 mM $CaCl_2$ in BES-buffered saline. Cells were incubated in neurobasal medium containing 2% B27 supplement and the transfection mix for 2.5 h in the presence of 10 µM DNQX and 100 µM DL-AP5. Conditioned medium was reapplied after washing the cells in PBS. Neurons were used for imaging experiments 5 days after transfection (11–13DIV). siRNA transfection was performed by using HiPerFect reagent (Sigma).

Immunocytochemistry

Hippocampal neurons were fixed in the presence of 4% paraformaldehyde (PFA) in PBS and permeabilized with 0.1% Triton X-100. Cells were stained with primary antibodies overnight at 4°C. Primary antibodies were rabbit anti-CAPS1 (1:1000, kindly provided by Teiichi Furuichi, RIKEN Brain Science Institute, Japan; Sadakata et al., 2006), rabbit anti-ClC3 (also known as CLCN3) (1:1000, cat. no. 252003, Synaptic Systems, Germany), mouse anti-V0a1 (1:1000, sc-374475, Santa Cruz Biotechnology) and mouse anti-MAP2 (1:1000, MAB3418, Merck Chemicals, UK) antibodies. Secondary antibodies conjugated with Alexa Fluor 488 (1:1000), Alexa Fluor 555 (1:1000) and Alexa Fluor 633 (1:1000) (Life Technologies) were incubated at room temperature for 2 h.

Colocalization studies were performed using a confocal imaging system (LSM 780, Zeiss, Germany) attached to an upright fluorescence microscope (Axio examiner.Z1, Zeiss, Germany) equipped with 20× and 63× water immersion objectives (both NA 1.0, Zeiss, Germany). Green fluorescence was excited using the 488-nm laser line from an argon laser, and red or infrared fluorescence was excited using 543-nm or 633-nm laser lines from a helium/neon laser. Signals were detected by a photon multiplier using GaAsP-detector array or PMT detectors.

Live cell imaging and fluorescence microscopy

Transfected cells were transferred into a bath chamber (Luigs & Neumann, Germany) filled with HEPES solution (20 mM HEPES, 100 mM NaCl, 4 mM KCl, 1 mM Na_2HPO_4, 2 mM $CaCl_2$, 1 mM $MgCl_2$, 100 µM Glycine) and inspected with a fluorescence microscope (BX51W, Olympus, Melville, NY) using a 60× water immersion objective (LUMFI, NA 1.1, Olympus, Melville, NY). Wavelength selection was accomplished by using filter sets (Chroma Technology) for green (excitation, 470±20 nm; emission, 525±25 nm) and red (excitation, 572±17.5 nm; emission, 632±30 nm) fluorescence mounted on filter wheels. Image capture was performed using a CCD camera (CoolSnap HQ^2, 14bit dynamic range, PhotoMetrics, Huntington Beach, CA) controlled by VisiView software (Visitron Systems, Germany). Unless otherwise specified, the exposure times for recordings (between 0.3 and 1.5 s) were adjusted for every cell. Image acquisition rates ranged from 0.25 to 0.1 Hz (Brigadski et al., 2005).

BDNF–GFP release and related assays

Neurons transfected with plasmids co-expressing BDNF–GFP and either control or CAPS1 shRNA were prepared for live-cell imaging. After recording baseline fluorescence levels, BDNF–GFP release was stimulated by applying HEPES buffer containing 50 mM KCl (adjusted for equal osmolarity) to a single transfected cell by a local perfusion system (Hartmann et al., 2001). The superfusion system consisted of a multi-barreled application pipette containing control and depolarizing solutions with a common outlet and an opposed drain pipette, creating a laminar flow

of solution (Lessmann and Dietzel, 1995). The superfusion system was positioned at a distance of ~400 µm from the recorded cell allowing complete exchange of applied solutions within 10 s (Kolarow et al., 2007). Using this superfusion system we observed similar delays, kinetics, and timecourses of BDNF–GFP secretion to those described previously for depolarization-induced and electrically induced BDNF release in hippocampal neurons (Brigadski and Lessmann, 2014; Hartmann et al., 2001). At the end of a measurement, HEPES buffer containing 0.3 mM BPB was superfused to discriminate content release from re-acidification. In some experiments, BDNF–GFP release was performed in the presence of 1 µM bafilomycin to eliminate the pH-sensitive response of GFP after vesicle fusion. Negative controls were obtained by analyzing closed BDNF-containing granules showing no change in fluorescence intensity throughout the recording. Kinetics of vesicle fusion events were measured by applying HEPES buffer containing 50 mM KCl in the presence of 0.3 mM BPB. Single-vesicle fusion events were observed by immediate quenching of GFP fluorescence after fusion pore opening (Kolarow et al., 2007). Either dendritic regions or single vesicles were analyzed for each measurement.

Fusion of BDNF-containing granules and release of BDNF was analyzed either in the absence or in the presence of synaptic blockers (5 µM DNQX, 50 µM DL-AP5 or 100 µM picrotoxin). Given that both release and fusion pore opening were indistinguishable in the presence or absence of synaptic blockers, data for both conditions were pooled.

FM® 1-43 destaining assay

Neurons were transfected with mCherry-expressing variants of the respective shRNA plasmids and stained with 10 µM FM® 1-43 (Invitrogen) by inducing depolarization for 2 min in HEPES buffer containing 50 mM KCl. Cells were washed in Ca^{2+}-free HEPES buffer and prepared for live-cell imaging. Neurons transfected with the respective shRNA construct were selected to record baseline fluorescence levels from active, FM® 1-43-stained synaptic boutons. Afterwards, cells were stimulated with HEPES buffer containing 50 mM KCl to record the destaining of FM® 1-43 (Klau et al., 2001).

Live-cell pH titration

Neurons transfected with either BDNF–GFP or GFP and the respective shRNA constructs were prepared for live-cell imaging. Cells were superfused with HEPES-buffered saline to record the baseline fluorescence intensity of single vesicles or dendritic stretches. Afterwards, a live-cell pH titration curve was obtained by perfusing cells with different MES or HEPES buffers containing 100 mM KCl, 10 µM nigericin and 4 µM valinomycin. To prevent BDNF–GFP release under these conditions, Ca^{2+}-free buffers were used. The pH values of buffers ranged from 4.0 to 8.0. Cells were superfused with a respective solution until the fluorescence change reached a plateau. Plateau values of 8–16 regions of interest (ROIs) per cell were averaged and fitted for sigmoid plots using the Boltzmann function of Origin software (OriginLab, Northampton, MA).

Image processing

Image analysis was performed using MetaMorph software (Universal Imaging Corporation, West Chester, PA). Between 8 and 20 ROIs (single vesicles or dendritic branches) were selected to cover the average change in fluorescence intensity of a single cell. Background fluorescence intensities were subtracted for each region and the average intensity was normalized to the time point before stimulation or treatment. A monoexponential extrapolation of the photobleaching observed during baseline recordings was applied to correct the normalized fluorescence data (Brigadski et al., 2005). Single-cell fluorescence data were averaged to obtain the mean fluorescence intensity changes (BDNF–GFP release and related assays and live-cell pH titration).

Statistical analysis

Statistical analysis was performed using SPSS version 22 software (IBM). All statistical analysis were performed using one-way ANOVA, followed by post hoc Tukey's HSD test. Statistical significance was determined as $P<0.05$.

The sample size was calculated with G-Power (University of Düsseldorf, Germany) based on previous reports. A total sample size of ten cultures was calculated given a significance level (alpha) of 0.05, a power of 0.95 and an effect size of 1.4. A random collection of our data was reanalyzed in a blind manner by a person not involved in the experiment. Comparison of this second independent analysis with the previous analysis revealed a high degree of correlation with an *r*-value >0.8.

Acknowledgements

We would like to thank Thomas Munsch and Kurt Gottmann for valuable suggestions and discussions, Nicola Ternette for critical reading of the manuscript, Sabine Mücke, Regina Ziegler, Margit Schmidt and Anja Reupsch for expert technical assistance, Gero Miesenböck (Department of Physiology, University of Oxford, UK) for kindly providing the synapto-pHluorin construct, and Teiichi Furuichi for kindly providing the CAPS1-YPet plasmid and the anti-CAPS1 antibody.

Competing interests

The authors declare no competing or financial interests.

Author contributions

Experiments were performed by R.E. The data were analyzed by R.E. and T.B. All authors designed experiments and wrote the manuscript. The study was designed and supervised by V.L. and T.B.

Funding

This work was funded by the German Research Foundation (DFG) [GRK 1167; SFB 779] and Leibniz Graduate School (LGS) on SynaptoGenetics to T.B. and V.L. The funders had no role in study design, data collection and analysis, decision to publish, or preparation of the manuscript.

Supplementary information

Supplementary information available online at
http://jcs.biologists.org/lookup/suppl/doi:10.1242/jcs.178251/-/DC1

References

Ann, K., Kowalchyk, J. A., Loyet, K. M. and Martin, T. F. (1997). Novel Ca2+-binding protein (CAPS) related to UNC-31 required for Ca2+-activated exocytosis. *J. Biol. Chem.* **272**, 19637-19640.

Boron, W. F. and De Weer, P. (1976). Intracellular pH transients in squid giant axons caused by CO2, NH3, and metabolic inhibitors. *J. Gen. Physiol* **67**, 91-112.

Brigadski, T. and Lessmann, V. (2014). BDNF: a regulator of learning and memory processes with clinical potential. *e-Neuroforum* **5**, 1-11.

Brigadski, T., Hartmann, M. and Lessmann, V. (2005). Differential vesicular targeting and time course of synaptic secretion of the mammalian neurotrophins. *J. Neurosci.* **25**, 7601-7614.

Brunk, I., Blex, C., Speidel, D., Brose, N. and Ahnert-Hilger, G. (2009). Ca2+-dependent activator proteins of secretion promote vesicular monoamine uptake. *J. Biol. Chem.* **284**, 1050-1056.

Dean, C., Liu, H., Dunning, F. M., Chang, P. Y., Jackson, M. B. and Chapman, E. R. (2009). Synaptotagmin-IV modulates synaptic function and long-term potentiation by regulating BDNF release. *Nat. Neurosci.* **12**, 767-776.

Deriy, L. V., Gomez, E. A., Jacobson, D. A., Wang, X., Hopson, J. A., Liu, X. Y., Zhang, G., Bindokas, V. P., Philipson, L. H. and Nelson, D. J. (2009). The granular chloride channel ClC-3 is permissive for insulin secretion. *Cell Metab.* **10**, 316-323.

Edelmann, E., Lessmann, V. and Brigadski, T. (2014). Pre- and postsynaptic twists in BDNF secretion and action in synaptic plasticity. *Neuropharmacology* **76**, 610-627.

Edelmann, E., Cepeda-Prado, E., Franck, M., Lichtenecker, P., Brigadski, T. and Lessmann, V. (2015). Theta burst firing recruits BDNF release and signaling in postsynaptic CA1 neurons in spike-timing-dependent LTP. *Neuron* **86**, 1041-1054.

Farina, M., van de Bospoort, R., He, E., Persoon, C. M., van Weering, J. R. T., Broeke, J. H., Verhage, M. and Toonen, R. F. (2015). CAPS-1 promotes fusion competence of stationary dense-core vesicles in presynaptic terminals of mammalian neurons. *eLife* **4**, e12968.

Fujita, Y., Xu, A., Xie, L., Arunachalam, L., Chou, T.-C., Jiang, T., Chiew, S.-K., Kourtesis, J., Wang, L., Gaisano, H. Y. et al. (2007). Ca2+-dependent activator protein for secretion 1 is critical for constitutive and regulated exocytosis but not for loading of transmitters into dense core vesicles. *J. Biol. Chem.* **282**, 21392-21403.

Grishanin, R. N., Kowalchyk, J. A., Klenchin, V. A., Ann, K., Earles, C. A., Chapman, E. R., Gerona, R. R. L. and Martin, T. F. J. (2004). CAPS acts at a prefusion step in dense-core vesicle exocytosis as a PIP2 binding protein. *Neuron* **43**, 551-562.

Harata, N. C., Choi, S., Pyle, J. L., Aravanis, A. M. and Tsien, R. W. (2006). Frequency-dependent kinetics and prevalence of kiss-and-run and reuse at

hippocampal synapses studied with novel quenching methods. *Neuron* **49**, 243-256.
Hartmann, M., Heumann, R. and Lessmann, V. (2001). Synaptic secretion of BDNF after high-frequency stimulation of glutamatergic synapses. *EMBO J.* **20**, 5887-5897.
Haubensak, W., Narz, F., Heumann, R. and Lessmann, V. (1998). BDNF-GFP containing secretory granules are localized in the vicinity of synaptic junctions of cultured cortical neurons. *J. Cell Sci.* **111**, 1483-1493.
Hay, J. C. and Martin, T. F. (1992). Resolution of regulated secretion into sequential MgATP-dependent and calcium-dependent stages mediated by distinct cytosolic proteins. *J. Cell Biol.* **119**, 139-151.
Henry, J. P., Botton, D., Sagne, C., Isambert, M. F., Desnos, C., Blanchard, V., Raisman-Vozari, R., Krejci, E., Massoulie, J. and Gasnier, B. (1994). Biochemistry and molecular biology of the vesicular monoamine transporter from chromaffin granules. *J. Exp. Biol.* **196**, 251-262.
Huang, E. J. and Reichardt, L. F. (2001). Neurotrophins: roles in neuronal development and function. *Annu. Rev. Neurosci.* **24**, 677-736.
Jockusch, W. J., Speidel, D., Sigler, A., Sørensen, J. B., Varoqueaux, F., Rhee, J.-S. and Brose, N. (2007). CAPS-1 and CAPS-2 are essential synaptic vesicle priming proteins. *Cell* **131**, 796-808.
Klau, M., Hartmann, M., Erdmann, K. S., Heumann, R. and Lessmann, V. (2001). Reduced number of functional glutamatergic synapses in hippocampal neurons overexpressing full-length TrkB receptors. *J. Neurosci. Res.* **66**, 327-336.
Klein, R. (1994). Role of neurotrophins in mouse neuronal development. *FASEB J.* **8**, 738-744.
Kneen, M., Farinas, J., Li, Y. and Verkman, A. S. (1998). Green fluorescent protein as a noninvasive intracellular pH indicator. *Biophys. J.* **74**, 1591-1599.
Kohara, K., Kitamura, A., Morishima, M. and Tsumoto, T. (2001). Activity-dependent transfer of brain-derived neurotrophic factor to postsynaptic neurons. *Science* **291**, 2419-2423.
Kolarow, R., Brigadski, T. and Lessmann, V. (2007). Postsynaptic secretion of BDNF and NT-3 from hippocampal neurons depends on calcium calmodulin kinase II signaling and proceeds via delayed fusion pore opening. *J. Neurosci.* **27**, 10350-10364.
Lessmann, V. and Brigadski, T. (2009). Mechanisms, locations, and kinetics of synaptic BDNF secretion: an update. *Neurosci. Res.* **65**, 11-22.
Lessmann, V. and Dietzel, I. D. (1995). Two kinetically distinct 5-hydroxytryptamine-activated Cl- conductances at Retzius P-cell synapses of the medicinal leech. *J. Neurosci.* **15**, 1496-1505.
Lessmann, V. and Heumann, R. (1998). Modulation of unitary glutamatergic synapses by neurotrophin-4/5 or brain-derived neurotrophic factor in hippocampal microcultures: presynaptic enhancement depends on pre-established paired-pulse facilitation. *Neuroscience* **86**, 399-413.
Matsuda, N., Lu, H., Fukata, Y., Noritake, J., Gao, H., Mukherjee, S., Nemoto, T., Fukata, M. and Poo, M.-m. (2009). Differential activity-dependent secretion of brain-derived neurotrophic factor from axon and dendrite. *J. Neurosci.* **29**, 14185-14198.
Nimmervoll, B., Flucher, B. E. and Obermair, G. J. (2013). Dominance of P/Q-type calcium channels in depolarization-induced presynaptic FM dye release in cultured hippocampal neurons. *Neuroscience* **253**, 330-340.
Park, H. and Poo, M.-M. (2013). Neurotrophin regulation of neural circuit development and function. *Nat. Rev. Neurosci.* **14**, 7-23.
Pyle, J. L., Kavalali, E. T., Piedras-Rentería, E. S. and Tsien, R. W. (2000). Rapid reuse of readily releasable pool vesicles at hippocampal synapses. *Neuron* **28**, 221-231.
Ryan, T. A., Reuter, H., Wendland, B., Schweizer, F. E., Tsien, R. W. and Smith, S. J. (1993). The kinetics of synaptic vesicle recycling measured at single presynaptic boutons. *Neuron* **11**, 713-724.
Sadakata, T., Itakura, M., Kozaki, S., Sekine, Y., Takahashi, M. and Furuichi, T. (2006). Differential distributions of the Ca2+-dependent activator protein for secretion family proteins (CAPS2 and CAPS1) in the mouse brain. *J. Comp. Neurol.* **495**, 735-753.
Sadakata, T., Kakegawa, W., Shinoda, Y., Hosono, M., Katoh-Semba, R., Sekine, Y., Sato, Y., Tanaka, M., Iwasato, T., Itohara, S. et al. (2013). CAPS1 deficiency perturbs dense-core vesicle trafficking and Golgi structure and reduces presynaptic release probability in the mouse brain. *J. Neurosci.* **33**, 17326-17334.
Sadakata, T., Kakegawa, W., Shinoda, Y., Hosono, M., Katoh-Semba, R., Sekine, Y., Sato, Y., Saruta, C., Ishizaki, Y., Yuzaki, M. et al. (2014). Axonal localization of Ca2+-dependent activator protein for secretion 2 is critical for subcellular locality of brain-derived neurotrophic factor and neurotrophin-3 release affecting proper development of postnatal mouse cerebellum. *PLoS ONE* **9**, e99524.
Shinoda, Y., Sadakata, T., Nakao, K., Katoh-Semba, R., Kinameri, E., Furuya, A., Yanagawa, Y., Hirase, H. and Furuichi, T. (2011). Calcium-dependent activator protein for secretion 2 (CAPS2) promotes BDNF secretion and is critical for the development of GABAergic interneuron network. *Proc. Natl. Acad. Sci. USA* **108**, 373-378.
Speidel, D., Varoqueaux, F., Enk, C., Nojiri, M., Grishanin, R. N., Martin, T. F. J., Hofmann, K., Brose, N. and Reim, K. (2003). A family of Ca2+-dependent activator proteins for secretion: comparative analysis of structure, expression, localization, and function. *J. Biol. Chem.* **278**, 52802-52809.
Speidel, D., Bruederle, C. E., Enk, C., Voets, T., Varoqueaux, F., Reim, K., Becherer, U., Fornai, F., Ruggieri, S., Holighaus, Y. et al. (2005). CAPS1 regulates catecholamine loading of large dense-core vesicles. *Neuron* **46**, 75-88.
Speidel, D., Salehi, A., Obermueller, S., Lundquist, I., Brose, N., Renström, E. and Rorsman, P. (2008). CAPS1 and CAPS2 regulate stability and recruitment of insulin granules in mouse pancreatic beta cells. *Cell Metab.* **7**, 57-67.
Südhof, T. C. (2005). CAPS in search of a lost function. *Neuron* **46**, 2-4.
Sugita, S. (2008). Mechanisms of exocytosis. *Acta Physiol.* **192**, 185-193.
Walent, J. H., Porter, B. W. and Martin, T. F. J. (1992). A novel 145 kd brain cytosolic protein reconstitutes Ca(2+)-regulated secretion in permeable neuroendocrine cells. *Cell* **70**, 765-775.
Wu, M. M., Grabe, M., Adams, S., Tsien, R. Y., Moore, H.-P. H. and Machen, T. E. (2001). Mechanisms of pH regulation in the regulated secretory pathway. *J. Biol. Chem.* **276**, 33027-33035.